JOURNAL DE PHYSIQUE IV
Colloque C2, supplément au Journal de Physique III, Volume 5, février 1995

A Random Field 3-State Spin Model to Simulate Hysteresis and Avalanches in Martensitic Transformations

J. Goicoechea and J. Ortín

Departament ECM, Facultat de Física, Universitat de Barcelona, Diagonal 647, 08028 Barcelona, Catalonia, Spain

Abstract: We propose a 3-state spin model to simulate the martensitic transition (MT) between austenite ($S = 0$) and two different, twin-related, martensitic phases ($S = \pm 1$). The system can be driven by two fields: Δ plays the role of temperature (drives the thermally-induced transition) and H plays the role of an uniaxial stress. Every spin S, in addition, experiences the effect of a static field h, randomly varying from site to site.
The model reproduces the avalanche-like kinetics of the MT and the shape of hysteresis cycles. We obtain the phase diagram of the model, study the evolution of χ (amount of martensite) and m (total strain) when the system is driven by the two external fields, and discuss the return-point memory properties of the trajectories. Finally, we study the role played by the random field on the statistical distribution of avalanches.

1. INTRODUCTION

From a number of experimental observations, the kinetics of thermoelastic martensitic transformations (MT) can be described in the following terms [1]: On driving the system with an external field, it follows a sequence of metastable two-phase state configurations. Each of them is a relative energy minimum, in which the system is momentarily trapped by the building up of elastic strain energy, until the driving field (that modifies the energy scenario) makes the configuration of the system to become unstable again;. this triggers an avalanche of non-equlibrium jumps until a new metastable configuration is reached. In this picture of the MT, it is worth noting that:
1. There are two different time scales: the duration of an avalanche is orders of magnitude smaller than the time spent in metastable equilibrium.
2. The passage from metastable to metastable equilibrium is accompanied by energy dissipation, and consequently the transformation-retransformation trajectories form a hysteresis cycle.
3. The energy barriers separating different metastable configurations are high compared to the energy of thermal fluctuations. In practice this means that thermal fluctuations do not play a significant kinetic role in the MT and, therefore, it is meaningful (a) to simulate the MT at 0 K and (b) to consider that the alloy temperature plays a role identical to an external driving field. This is also the reason for the reproducible behaviour of the system from cycle to cycle. An extreme example of such reproducibility is the return-point memory (RPM) property, observed for several martensitic alloy systems under different kinds of solicitation [2].

The purpose of this paper is to introduce and study a toy model of the MT which, deliberately, ignores the fundamental physics of the transition (not yet well understood) but captures almost all the interesting kinetic features of the transition summarized above. The paper is organized in the following way: the model and the simulation algorithm are explained in section 2. The phase diagram of the model in terms of the fields Δ and H is presented in section 3, together with typical transformation trajectories. Section 4 presents a statistical analysis of the transformation avalanches. Finally, the relevance of these results, in connection with the kinetics of the MT, is discussed in section 5.

2. MODEL AND SIMULATION ALGORITHM

Our 3-state spin model consists of an $N \times N$ square lattice with a spin state variable $S(x,y) = +1, 0, -1$ defined on each lattice site. The spin value $S(x,y) = 0$ represents the austenitic (parent) phase, and the values $S(x,y) = \pm 1$ two martensitic phases related by a twin operation in two dimensions. In a sense, the value of $S(x,y)$ represents the transformation strain on each lattice site in two dimensions. A configuration of the model is given by the ensemble $\{S(x,y)\}$ for all lattice sites. Elastic interactions between different domains are modeled by nearest neighbours interactions, with periodic boundary conditions to avoid artificial boundary effects. Three different values of the interaction energies have been considered:

$K_{mm'}$: energy between two differently oriented martensitic domains.

K_{ma}: energy between martensite and austenite domains.

K_e: energy between two domains of the same type.

Therefore, the *local* interaction energy for a site (x,y) with spin value $S(x,y)$ is given by

$$\begin{aligned}\mathcal{H}(x,y) = &-K_{mm'}[\delta_{S(x,y),1} \sum_{<u,v>} \delta_{S(u,v),-1} + \delta_{S(x,y),-1} \sum_{<u,v>} \delta_{S(u,v),1}] \\ &-K_{ma}[\delta'_{S^2(x,y),1} \sum_{<u,v>} \delta'_{S^2(u,v),0} + \delta'_{S^2(x,y),0} \sum_{<u,v>} \delta'_{S^2(u,v),1}] \\ &-K_e[\delta_{S(x,y),1} \sum_{<u,v>} \delta_{S(u,v),1} + \delta_{S(x,y),1} \sum_{<u,v>} \delta_{S(u,v),-1} + \delta_{S(x,y),0} \sum_{<u,v>} \delta_{S(u,v),0}] \\ &-H \cdot S(x,y) + \Delta \cdot S^2(x,y)\end{aligned}$$

where

$$\begin{aligned}&\delta_{x,1} = \tfrac{1}{2}x(1+x) && \delta'_{x,1} = x \\ &\delta_{x,-1} = -\tfrac{1}{2}x(1-x) && \delta'_{x,0} = 1-x \\ &\delta_{x,0} = 1-x^2\end{aligned}$$

and $< u,v >$ indicates summation over the 4 nearest neighbours of the site (x,y). Every spin $S(x,y)$ wants to take the value that minimizes the local interaction energy $\mathcal{H}(x,y)$. Hence, given that all the interaction terms are preceded by a negative sign, the higher an interaction energy the more favoured is the configuration associated with that interaction. In addition, we have introduced two external fields Δ and H. Δ couples to S^2, and therefore a positive Δ favours $S(x,y) = 0$, while a negative Δ favours $S(x,y) = \pm 1$, without distinction; in this sense, Δ plays the role of a temperature in the MT. Since, on its turn, H couples to S, a positive H favours $S(x,y) = 1$ and a negative H favours $S(x,y) = -1$; thus, H breaks the degeneracy between the two martensitic orientations and, in this sense, acts as an uniaxial stress field in the MT.

Conjugate to these two fields, we define two order parameters:

$$\chi = \sum_{(x,y)} S^2(x,y) \qquad \text{(total amount of martensite)}$$

$$m = \sum_{(x,y)} S(x,y) \qquad \text{(total strain)}$$

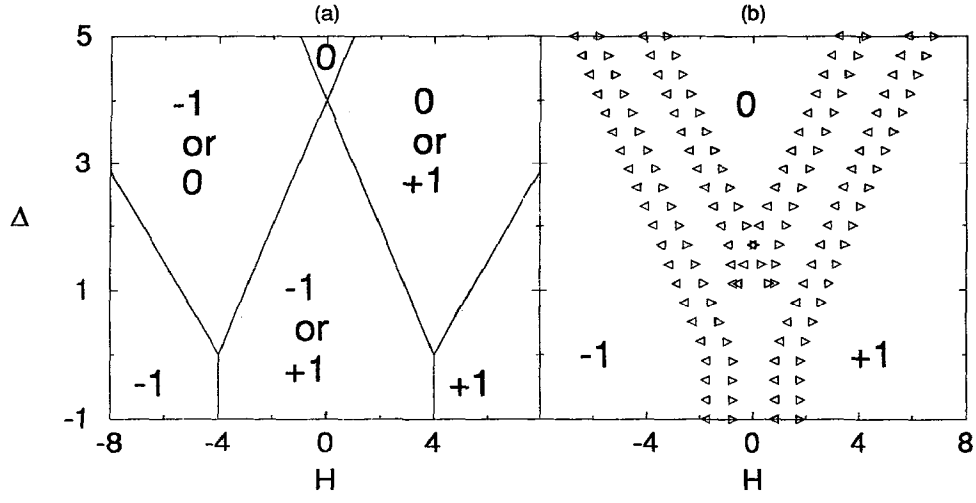

Figure 1. Phase diagrams obtained by increasing and decreasing H at constant Δ. (a) $\sigma = 0$. Shown are the boundary lines separating different homogeneous phases; the Y at the right (left) side corresponds to increasing (decreasing) H. (b) $\sigma = 2$. Each point in the phase diagram is computed from statistical averages on 100 runs for a system of 40×40 sites; the previous boundary lines become now Y-shaped coexistence regions; triangles pointing to the right (left) represent paths of increasing (decreasing) H. The size of the symbols accounts for the error bars.

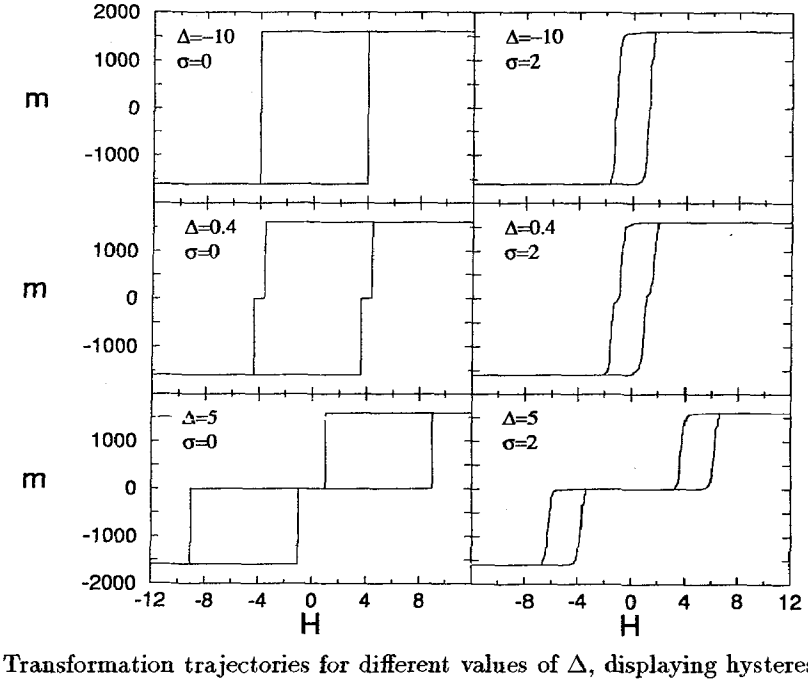

Figure 2. Transformation trajectories for different values of Δ, displaying hysteresis. $\sigma = 0$ corresponds to the BEG model and $\sigma = 2$ to the RFBEG model.

where (x, y) indicates summation over all sites of the system.
After some algebra, the local interaction energy can also be written in the following form:

$$\mathcal{H}(x,y) = -4K_e - \tfrac{1}{2}\Delta_{mm'} \sum_{<u,v>} S(x,y)S(u,v) - (2\Delta_{ma} - \tfrac{1}{2}\Delta_{mm'}) \sum_{<u,v>} S^2(x,y)S^2(u,v)$$
$$+(\Delta + 4\Delta_{ma}) \cdot S^2(x,y) + \Delta_{ma} \sum_{<u,v>} S^2(u,v) - H \cdot S(x,y)$$

where $\Delta_{mm'} = K_e - K_{mm'}$ and $\Delta_{ma} = K_e - K_{ma}$. This other form of writing $\mathcal{H}(x, y)$ shows how the interaction terms group in two different kinds: those that only involve S, and therefore distinguish between the two martensite orientations, and those that only involve S^2 and hence do not make the distinction. Written in this form, the model is reminiscent of a Blume-Emery-Griffiths (BEG) spin model [3].
The so-called *random field* version of our model (RFBEG) is obtained by adding to the external field H a local field $h(x, y)$ that takes a *random* value on each lattice site. The distribution used for $h(x, y)$ is a gaussian with mean value 0 and variance σ.
The evolution of the model, driven by one of the two external fields (while the other field remains constant), is simulated in the following way: starting from a well defined configuration (e.g. $S(x, y) = -1$ at all sites, $\Delta \ll 0$, $H \ll 0$) the field is changed in a single step up to the value at which at least one spin becomes locally unstable. All the unstable spins are then simultaneously changed to their stable configurations (synchronous updating). Without modifying the external field, the process is iterated (an avalanche develops) until all the spins are locally stable. The overall process is then repeated starting from this new metastable configuration. This algorithm gives rise to *adiabaticity* in the dynamics, i.e. the actual rate of evolution of the driving field is irrelevant since, at each step, a whole avalanche is completed without any appreciable variation of the field.

3. PHASE DIAGRAM AND HYSTERESIS CYCLES

The phase diagram of the BEG model, neglecting thermal fluctuations ($0K$), is shown in figure 1(a). Here $\sigma = 0$ (there is no random field), and the system can only be found in three different homogeneous phases: $S(x, y) = +1\ \forall(x, y)$, $S(x, y) = 0\ \forall(x, y)$, $S(x, y) = -1\ \forall(x, y)$. The transitions between these three phases take place abruptly, through a giant avalanche that sweeps the whole system. Due to the spin-spin interaction, there are two parallel phase boundary lines for each transition, one for increasing H and another for decreasing H. This gives rise to hysteresis in the transformation trajectories, as shown in figure 2.
The phase diagram of the RFBEG model (including now a random field of variance $\sigma = 2$), again at $0K$, is presented in figure 1(b). The system exhibits hysteresis, and hence there are again two boundaries for each transition. This time, however, the boundaries are no longer well-defined lines in the phase diagram because, in addition to the three homogeneous phases, the system can be found in metastable two-phase (or even three-phase) states: the boundaries become regions of finite width (associated with the range of driving fields in which two or three phases coexist). The phase diagram can be viewed as the overlap of two wide Y-shaped regions, one corresponding to transitions of increasing H and the other to transitions of decreasing H.
The corresponding transformation trajectories are shown in figure 2; since the random field makes the system heterogeneous, the transformation in different lattice sites takes place at different values of the driving field; this effect, combined with the spin-spin interactions, gives rise to avalanches of varying sizes along the transformation trajectories. For $\Delta \ll 0$ the austenitic phase is unstable, the system is fully martensitic, and the orientation of the martensite domains is determined by their mutual interactions and the external stress field H. In this range of Δ the model coincides exactly with a random field Ising model (RFIM) [4], because $S = \pm 1$ and the square terms (S^2, $S^2 \cdot S^2$) remain constant under changes of H. On the other hand, for $\Delta > 0$, above some positive value, the

austenitic phase ($S = 0$) becomes stable; in this range of Δ the martensitic domains can only appear by application of an external stress H. For intermediate values of Δ (around 0), the three phases coexist. This behaviour and the shape of simulated hysteresis cycles are consistent with experimental observations in real alloy systems.

Regarding the return-point memory (RPM) property, observed in a number of thermoelastic MT under different experimental conditions, our simulations show that a RFBEG model presents RPM in the martensitic region ($\Delta \ll 0$), where it coincides with a RFIM. However, the RPM property is not satisfied by transformation trajectories that simultaneously involve the austenitic and the two martensitic phases, presumably because the two martensitic phases are degenerated with respect to the field Δ. This aspect of the problem is currently under investigation.

4. AVALANCHE DISTRIBUTIONS

As shown above, the hysteresis cycles change with the amount of static disorder quenched in the system (parametrized by σ). In particular, for large σ the transformation events are practically uncorrelated (most of the spins change because of their own random field, independently of their neighbours) and the avalanches involve only a few spins, while for small σ the value of the random field is very similar in many lattice sites and hence the transformation in one site is correlated to transformation in many other sites, leading to very large avalanches.

Sethna *et al.* [4], in their investigation of the RFIM, showed that the passage from large σ to small σ involved a disorder-driven second-order phase transition. At the critical value of disorder, σ_c, the system developed avalanches of all sizes that followed a power-law distribution.

We have carried out this same investigation for the RFBEG model [5], simulating Δ-induced transformations, at $H = 0$, for different values of σ; For each σ we have performed 500 runs with different random seeds to provide for good statistics. We have decreased Δ from the region where the austenitic phase is stable down to the region where the stable phases are martensitic and looked, along the transformation, for the largest jump in the two order parameters χ and m (largest avalanche) and for the time τ_{max} elapsed in the avalanche of longest duration. As a function of σ, $\mid \Delta\chi \mid_{max}$ and $\mid \Delta m \mid_{max}$ present inflection points at the critical point, while τ_{max} presents a maximum. The critical exponents of the disorder-driven transition can be evaluated by repeating this procedure for different system sizes and performing a finite-size scaling analysis. The exponential behaviour near σ_c is given, at $H = 0$, by:

$$\mid \Delta\chi \mid_{max} \sim \mid (\sigma - \sigma_c)/\sigma_c \mid^{D}$$

$$\mid \Delta m \mid_{max} \sim \mid (\sigma - \sigma_c)/\sigma_c \mid^{D'}$$

$$\tau_{max} \sim \mid (\sigma - \sigma_c)/\sigma_c \mid^{z}$$

The exponents obtained are $D = 2.2 \pm 0.1$, $D' = 2.3 \pm 0.1$ and $z = 1.3 \pm 0.1$. The critical value of disorder is found to be $\sigma_c = 0.51 \pm 0.03$

5. DISCUSSION AND CONCLUSIONS

The model studied in this paper belongs to a family of spin models recently designed to simulate and analyze the kinetic features of fluctuationless phase transitions. They all share the property of incorporating some kind of frozen-in disorder. This kind of approach has been pioneered by Sethna *et al.* [4], in their study of the RFIM driven by a magnetic field, and continued by Vives and Planes [6] in their work on the random-bond Ising model (RBIM). The RFBEG model presented here introduces the novelty of a 3-state spin variable, representing austenite and two twin-related martensitic phases, and the possibility of two external driving fields that have distinct effects on the different

phases. In this sense the RFBEG model is particularly suitable to model a thermoelastic martensitic transition, driven by temperature and uniaxial stress.
In the region $\Delta \ll 0$ the RFBEG model behaves as a 2-state spin model and gives rise to identical results than the RFIM. The simulated trajectories reproduce experimental cycles of stress-induced martensite reorientation. However, for intermediate and large values of Δ, the possibility of an austenitic phase gives rise to new kinds of trajectories. In the region of large Δ, where the martensitic phases can only be stress-induced, the simulated trajectories qualitatively reproduce pseudoelastic cycles of single crystals under tension and compression.
The three main ingredients of the model (nearest neighbours interactions between spins, static random field acting on each spin, absence of fluctuations) give rise to *avalanche kinetics*, consistent with experimental observations. In this context, recent experimental studies [7] of the acoustic emission detected in the thermally-induced transformation of a CuZnAl alloy have shown that the amplitude and time duration of the transformation avalanches distribute according to power-laws, with no characteristic amplitude or time scale. This observation is, without doubt, closely related to the self-similar character (absence of characteristic length scales) of martensitic microstructures.
In the RFBEG model, however, the avalanches corresponding to thermally-induced transformations (Δ excursions at constant H) distribute according to a power-law only for a critical value of the static disorder. If we accept that the model captures the essential kinetic features of the transformation, the question is how the actual alloy system can be attracted towards such a particular value of static disorder. It has been speculated that the defect rearrangement that takes place during the first few cycles following an annealing treatment in the austenite phase could spontaneously drive the system to the critical value of disorder. In this sense, let us recall that the CuZnAl crystal used in the experiments reported above had been subjected to repetitive thermal cycling before reaching a stable hysteresis cycle with reproducible power-law statistics.
At this point, it is worth noting that the topological features of martensite and austenite domains are missing in the models mentioned. The crystal degeneracy of the martensitic phase (24 variants) favours topological defects at phase boundaries that, probably, as they do in other systems evolving by avalanches [8], play a relevant role in the kinetics of the MT.

ACKNOWLEDGEMENTS

This work has received financial support from the CICyT, project nr. MAT92-884. The authors acknowledge the Centre de Super Computaci de Catalunya (CESCA) for using their computing facilities.

REFERENCES

[1] Khachaturyan A.G., Theory of Structural transformations in Solids (Wiley, New York, 1983).
[2] Ortín J., *J. Appl. Phys.* **71** (1992) 1454, and references therein.
[3] Blume M., Emery V.J., Griffiths R.B., *Phys. Rev. A* **4** (1971) 1071.
[4] Sethna J.P., Dahmen K., Kartha S., Krumhansl J.A., Roberts B.W., Shore J.D., *Phys. Rev. Lett.* **70** (1993) 3347.
[5] Vives E., Goicoechea J., Ortín J., Planes A., to be published.
[6] Vives E., Planes A., *Phys. Rev. B* **50** (1994) (in press); see also these Proceedings.
[7] Vives E., Ortín J., Mañosa Ll., Ràfols I., Pérez-Magrané R., Planes A., *Phys. Rev. Lett.* **72** (1994) 1694.
[8] Weaire D., Bolton F., Molho P., Glazier J.A., *J. Phys.: Condens. Matter* **3** (1991) 2101.